Journal of The Electrochemical Society

Electrochemical Deposition and Characterization of Ni in Mesoporous Silicon

A. Dolgiy, S. V. Redko, H. Bandarenka, S. L. Prischepa, K. Yanushkevich, P. Nenzi, M. Balucani and V. Bondarenko

J. Electrochem. Soc. 2012, Volume 159, Issue 10, Pages D623-D627.
doi: 10.1149/2.050210jes

Email alerting service Receive free email alerts when new articles cite this article - sign up in the box at the top right corner of the article or click here

To subscribe to *Journal of The Electrochemical Society* go to:
http://jes.ecsdl.org/subscriptions

© 2012 The Electrochemical Society

Journal of The Electrochemical Society, **159** (10) D623-D627 (2012)
0013-4651/2012/159(10)/D623/5/$28.00 © The Electrochemical Society

Electrochemical Deposition and Characterization of Ni in Mesoporous Silicon

A. Dolgiy,[a] S. V. Redko,[a] H. Bandarenka,[a,*,z] S. L. Prischepa,[b] K. Yanushkevich,[c] P. Nenzi,[d] M. Balucani,[d] and V. Bondarenko[a]

[a]*Department of Micro- and Nanoelectronics, Belarusian State University of Informatics and Radioelectronics, Minsk 220013, Belarus*
[b]*Department of Telecommunications, Belarusian State University of Informatics and Radioelectronics, Minsk 220013, Belarus*
[c]*Scientific and Practical Materials Research Center of Belarusian Academy of Sciences, Minsk 220072, Belarus*
[d]*Department of Information Engineering, Electronics and Telecommunications, University of Roma "La Sapienza", Rome 00184, Italy*

Nickel nanowires have been formed by stationary electrochemical deposition of nickel into mesoporous silicon templates from the modified Watts bath. Monitoring of the porous silicon potential during the electrochemical deposition has given the determination of the emergence of Ni on the outer surface of porous layer. Maximum filling factor of porous silicon with Ni has been achieved to 67%. The pore dimensions have been found to define the length and diameter of the Ni nanowires that have equaled to 10 μm and 100–120 nm, respectively. The polycrystalline nature of the nickel nanowires, as well as the expansion of nickel lattice constant in comparison with bulk material has been established by analyzing the X-ray diffraction spectra. The synthesized samples have possessed ferromagnetic properties, which have been confirmed by temperature measurements of the magnetization. Smaller values of the specific magnetization of the Ni/PS samples and the atomic magnetic moment of Ni atoms at the low temperature with respect to those of bulk material have been suggested to be mostly caused by formation of nickel silicide at the beginning of the Ni electrochemical deposition.
© 2012 The Electrochemical Society. [DOI: 10.1149/2.050210jes] All rights reserved.

Manuscript submitted June 11, 2012; revised manuscript received July 20, 2012. Published August 29, 2012. This was Paper 835 presented at the Boston, Massachusetts, Meeting of the Society, October 9–14, 2011.

Nanowires (NWs) of ferromagnetic metals incorporated into porous templates of nonmagnetic materials have been the subject of an intensive research during the last decade as they may exhibit the giant magnetoresistance effect and coherent spin waves.[1,2] Because of the large aspect ratio (the ratio of the diameter of NWs to their length), the distinguishing feature of these nanoobjects is their high magnetic anisotropy. All these together make those promising for use in the perpendicular magnetic recording with high packing density.[3,4]

To date, many studies have been performed to obtain ferromagnetic NWs by using electrochemical deposition of metals in the porous anodic alumina templates[5,6] and in track etched polymer membranes.[7,8] Porous silicon (PS) templates provide additional unique features since the diameter of the pores and the porosity of the channels can be varied in a wider range than in case of porous anodic alumina and polymer membranes. In addition, the fabrication of PS and metal filling of the PS matrix are in good correspondence with the modern micro- and nanoelectronic technology requirements. Studies on the electrochemical deposition of ferromagnetic metals in the PS were started in the early 80's of the last century. The driving force behind this research was the idea of getting thick layers of silicide by filling the channels of PS with metal followed by thermal annealing. The first work on the electrochemical deposition of nickel in PS was published in 1985.[9] Several similar works have been carried out after that, which were summarized in a 1997 review.[10] The first results on the anisotropy of the magnetic properties of nickel nanowires in the matrix of PS were observed in 1994,[11] while the influence of the porosity of the PS template on the type of magnetic anisotropy was revealed only 15 years later.[12] Recently the critical analyzes of the current state-of-the-art of the employment of PS as a template for different magnetic nanocomposites have been presented.[13,14]

Apart from the aspect ratio a filling factor is another fundamental parameter of metallic NWs in the PS template. The filling factor is the ratio of the metal mass effectively deposited into the porous layer to the metal mass, which can be theoretically introduced into the pore channels of the template to provide a complete filling with metal. The magnetization and the anisotropy of magnetic properties are able to be improved by increasing both the aspect ratio and the filling factor. Obtained objects with the aspect ratio greater than 100 and the filling factor higher than 25% is still challenging.[14] Morphological changes of the pore walls like dendritic branches as well as hydrogen evolution lead to inhomogeneity of the metal deposit so it is very difficult to obtain homogeneous filling of the pores. If the exchange of reagents within the pore is limited the channel might be blocked by the accumulation of the deposited metal. This prevents uniform filling of the pores along its entire length. One possible way to overcome this problem is a pulsed electrochemical deposition of metal in PS. At the present time, use of a pulse mode allows forming of Ni NWs in the matrix of PS with diameters ranging from 20 nm to 100 nm and a length of several micrometers.[11,13,14]

In this work Ni deposition into pores of the mesoporous silicon under the stationary galvanostatic regime from a modified Watts bath has been investigated. We have fabricated PS samples of 72% porosity. As a result, the pores of 10 μm length and 100 nm of diameter have been surprisingly well filled with Ni without use of the pulsed mode.

Experimental

Antimony doped 100 mm monocrystalline silicon wafers with (100) orientation and 0.01 Ohm$\times$cm resistivity were used as the initial substrates. Chemical cleaning of the Si wafers was performed for 10 min with a hot (75°C) solution of NH_4OH, H_2O_2 and H_2O mixed in a volume ratio of 1:1:4. After that the wafers were rinsed in the deionized water and dried in a centrifuge. Then the wafers were cut into a number of rectangular 3$\times$3 cm samples. Just before PS formation each experimental sample was immersed into the 5% HF solution for 30 s to remove the native oxide. Immediately after the oxide removal, the Si sample was placed in an electrolytic cell made of Teflon. The active opening of the cell had a round shape and the area of 3 cm^2. Uniform PS layers were formed by electrochemical anodization of silicon samples in a solution of HF (45%), H_2O and $(CH_3)_2CHOH$ mixed in a 1:3:1 volume ratio. A spectrally pure graphite disk was used as a contact electrode to the back side of the samples during the electrochemical treatment. Platinum spiral wire was used as a cathode electrode. Anodization was performed at a current density of 80 mA/cm^2 for 200 s. This regime provided formation of the uniform PS layers with the 10 μm thickness and 72% porosity. Pore diameters of 100–120 nm and pore density of 2×10^{10} cm^{-2} were estimated from the SEM images.

* Electrochemical Society Active Member.
z E-mail: h.bandarenka@gmail.com

After PS formation the HF solution was removed and the electrolytic cell was thoroughly rinsed in the deionized water. The cell was then filled with an electrolyte for the nickel deposition. Nickel was incorporated into PS matrix by electrochemical deposition at the different constant current density values. However, we represented below the description of the structures formed at 3.5 mA/cm^2 as it resulted in the highest factor of PS filling with Ni. The composition of electrolyte for the Ni deposition was slightly different from that known for the Watts bath. It consisted of 213 g/L $NiSO_4\,7H_2O$, 5 g/L $NiCl_2.6H_2O$, 25 g/L H_3BO_3 and 3 g/L saccharin. At room temperature such electrolyte has pH=2.6. Ni was deposited on five PS samples for 5, 15, 30, 60 and 80 minutes. Potential measurements were carried out by use of the Ag/AgCl reference electrode filled with the saturated KCl solution. The reference electrode was immersed into a small bath filled with the solution for the Ni deposition. The bath was connected with the electrolytic cell by a flexible polymer tube of the 2 mm inner diameter ended with a Luggin glass capillary of 200 μm aperture. Both the Luggin capillary and polymer tube were filled with the solution for the Ni deposition. The Luggin capillary was placed on the surface of PS and defined a clear small sensing point for the reference electrode near the PS electrode.

The equipment used to conduct electrochemical process was the potentiostat/galvanostat AUTOLAB PGSTAT302n. Gravimetric method was applied to determine the porosity of PS and the filling factor of Ni. Mass measurements were performed with Sartorius CP225D micro/analytical electronic balance. The instrumental error of mass measurements was about 10 μg.

The structure of the samples was studied with the scanning electron microscope (SEM) Hitachi S-4800. The elemental composition in different selected points of the samples was determined using SEM Cambridge Instruments Stereoscan-360 with a Link Analytical AN 10000 energy dispersive X-ray analyzer. The diameter of the focused electron beam was less than 2 μm. The phase composition of the samples was determined by X-ray diffraction (XRD) using CuKα radiation (X-ray wavelength λ=0.15406 nm). The magnetic properties of the samples were studied by measuring the magnetization at the temperatures from 77 to 700 K by static ponderomotive method.[15]

Results and Discussion

Mechanism of PS filling with Ni.— One of the important tasks of the electrochemical deposition of metals into PS is the determination of the specific time points, which correspond to different filling stages. The moments of the initial precipitation of metal on the pore walls and the complete filling of the whole pore volume are especially important. To solve such problem the applied electrochemistry offers measurement of the potential of PS during the deposition in galvanostatic mode. The measurement of PS potential as a function of deposition time may provide considerable insight on the different deposition behaviors.[16]

Figure 1 shows the dependencies of the PS potential on Ni deposition time for five PS samples with 10 μm of porous layer thickness and 72% of porosity.

Measurement of the PS potential was started immediately after filling the cell with the electrolyte and the cathodic current was applied 10 minutes later. Ni was deposited in PS during different periods of time: 5, 15, 30, 60 and 80 minutes, as it is marked in Figure 1. After stop of the deposition (these points correspond to the decreasing spikes of the potential) the potential was recorded a while longer. The value of potential in the electrolyte without external polarization was almost constant in time and fluctuated around −0.475...−0.485 V. It indicates no appreciable change in reactions on PS surface, i.e. the surface of PS is stable in the Watts solution and does not change.[16] At the moment of the current turn-on the sharp increase of PS potential up to −0.975...−0.98 V was observed. Afterwards the potential is gradually reduced and in 12 min reached permanent value of about −0.83...−0.84 V. Half an hour later PS potential started again slow rising which stopped at 55–60 min at the value of −0.95 V. Further deposition did not change this value. Current turn-off at 5, 15 and 30 minutes (curves 1, 2 and 3) led to the immediate potential decreasing to −0.37...−0.375 V. The same reduction of the potential was observed after current stops at 60 and 80 minutes (curves 4 and 5, respectively) but it took more than 30 minutes to reach constant value of −0.38 V. Below it will be shown that such potential behavior after 60 min of the process indicates a full coverage of PS surface with Ni.

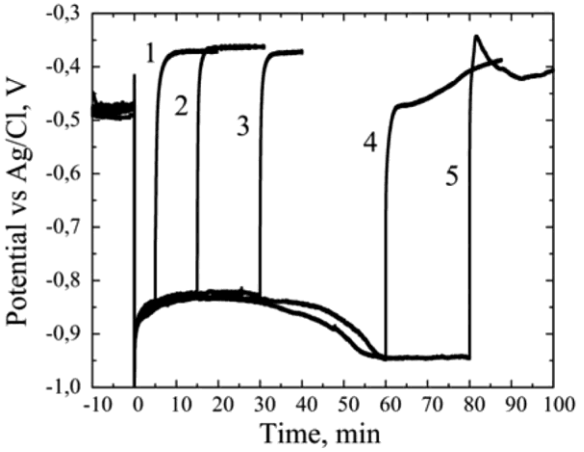

Figure 1. The potential of PS vs. time of nickel electrochemical deposition. Deposition process was stopped at different times: 5 (1), 15 (2), 30 (3), 60 (4), 80 (5) minutes.

To study the filling process of PS with Ni we have used SEM of cross sections of the experimental samples after different periods of the metal deposition. As an example, Figure 2 presents SEM images of the top, middle and bottom parts of cross sections for 5, 15 and

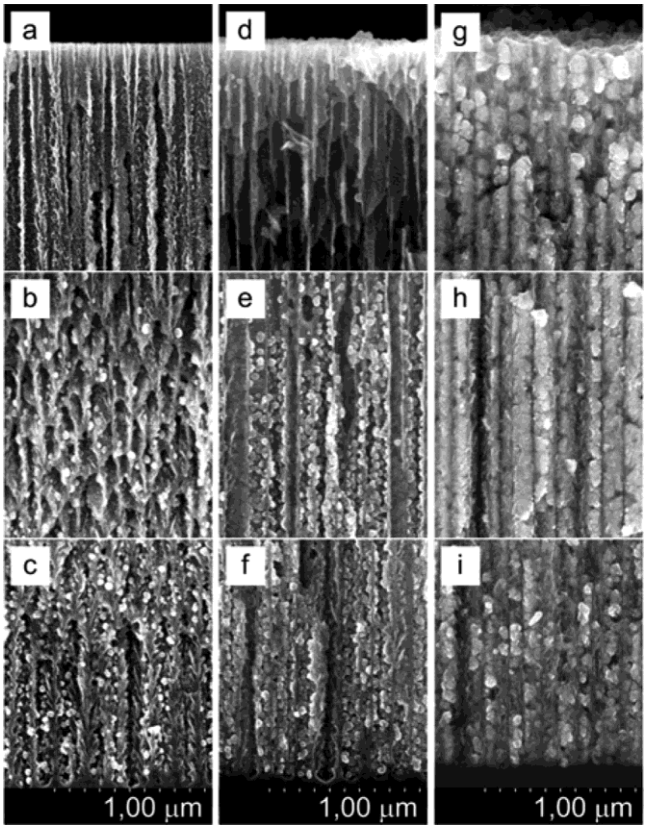

Figure 2. SEM images of the top (a, d, g), middle (b, e, h) and bottom (c, f, i) regions of cross sections of PS subjected to the Ni deposition for 5 (a, b, c), 15 (d, e, f) and 80 (g, h, i) minutes.

80 minutes samples. There are only a few nanoparticles (NPs) of nickel observed on the pore walls in the top area of the 5 min sample (Fig. 2a). In the central part of the 5 min sample (Fig. 2b) NPs of 30–50 nm in diameter are seen. The average linear density of NPs is about 5–7 per 1 μm of pore length. The bottom image of the 5 min sample (Fig. 2c) shows the interface between PS and monocrystalline Si. It is characterized by significant increase of NPs linear density to several tens per 1 μm. Such fact means that the metal deposition process began mostly in the lower part of the pore channels. The more careful analysis of the SEM images of the 5 minutes sample (Fig. 2a, 2b, 2c) reveals that the primary Ni NPs nucleation occurred on the tips of the PS skeleton branches. We suggest it was caused by high local current density due to accumulation of the electric field on the tiny ends of the PS elements. The pore entrances were not blocked as well as Ni deposition on the outer surface of PS did not take a place. The filling factor for the 5 minutes sample was estimated by gravimetric method as 4.5%.

Figure 2d, 2e, 2f shows SEM pictures of cross section of the 15 minutes sample. The top and the middle regions of PS (Fig. 2d, 2e) look like the same areas of the 5 minutes sample but are characterized by relatively larger density of NPs. However, in the bottom part we see great differences. The dimensions of Ni NPs are about 40–70 nm as in the center but their density is several times more. Moreover, Ni NPs coalesced and formed quasi continuous wires. The filling factor of the described sample was about 23%.

Figure 2g, 2h, 2i presents SEM cross sections images of the 80 minutes sample. The outer surface of the sample was covered with the continuous nickel film of 2 μm thickness. The upper Ni layer is not observed on Fig. 2g, because it was mechanically removed before the sample's cutting for the SEM analysis. Pore channels in this case are well filled with metal NWs which represent columns of the large tightly contacted conglomerates of nickel. On the top of the cross section grown together particles are observed. The diameter of the particles varies in the range from 100 to 120 nm. It should be noted that pretreatment of the sample, resulting in the exfoliation of the surface layer of Ni, could destroy the Ni NWs in the upper part of the sample. In the middle of the 80 minutes sample nickel NWs are rather monolithic and their diameters are about 100–120 nm. It exactly corresponds to the diameters of the pore channels. At the bottom of the 80 minutes sample the completeness of nickel filling is lower than in the central part. It is possible to see the individual NPs of nickel. The filling factor was estimated as 67%.

Detailed study of the kinetics of Ni deposition in the PS matrix required X-ray microanalysis of the cleavage surface of the samples. The profile of distribution of the Ni concentration from the surface to the bottom of the porous layer was obtained. Results of the analysis are shown in Figure 3. We analyzed the profiles of nickel in PS (Fig. 3) and data on the morphology of the samples (Fig. 2) for different times of Ni deposition and proposed the following mechanism of the nickel NWs growth.

The nucleation and growth of Ni NPs begin at the initial stages (less than 5 minutes) in the lower region of PS (in the depth of 8–10 μm from the surface) on the tips of branches of the PS skeleton. The diameters of NPs are around 40–70 nm. Prolongation of the deposition time to 15 minutes leads to the increase of the density of nickels NPs in the central and bottom parts of PS. It is mostly caused by increase in the number of Ni NPs than changing of their dimensions which grow very slightly. In that way Ni NPs coalesce and almost completely fill the pore channels with deposition for 60 minutes as it is proved by constant potential value 0.95 V (Fig. 1). Further deposition causes Ni continuous layer formation on the outer surface of PS (80 minutes).

The consideration of the obtained results allows summarizing the PS potential stabilization after 60 minutes of the Ni electrochemical deposition is related to the emergence of Ni from the porous layer on the outer surface of PS. In that way control of the PS filling level during the formation of Ni NWs in the PS template might be performed.

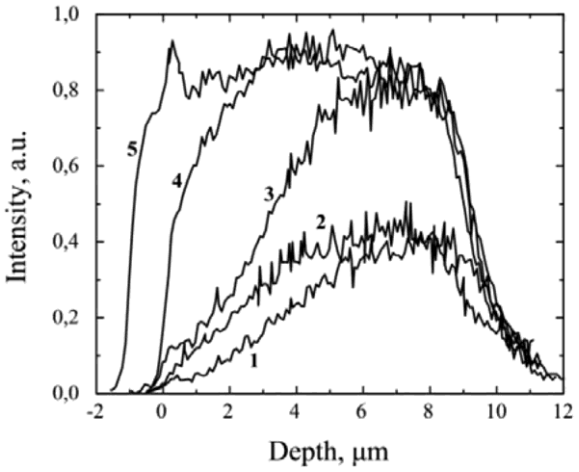

Figure 3. X-ray microanalysis profiles of the Ni distribution in PS subjected to the Ni electrochemical deposition for 5 (1), 15 (2), 30 (3), 60 (4) and 80 (5) minutes.

Crystalline structure of Ni deposited in PS.— XRD analysis was carried out to prove the crystalline nature of the Ni deposit in the PS templates. Figure 4 shows XRD patterns of PS after Ni electrochemical deposition for 5, 15 and 80 minutes.

It is known that crystalline nickel has cubic crystal cell with the lattice parameter a 0.3524 nm.[17] As seen from Figure 4, each diffraction pattern has reflexes corresponding to the major Ni crystallographic planes (111), (200) and (220). Such XRD spectra are typical for the electro-deposited polycrystalline Ni NWs.[18] Si substrate itself resulted in a peak of high intensity which appeared at the angle responsible for the silicon (400). Calculated lattice parameter a of Ni in PS is 0.4–0.5% higher than that of nickel powder and varies in the range from 0.3537 to 0.3541 nm. The expansion of the crystal lattice means that Ni in pores of PS is strained. Probably, it is caused by the affect of Si lattice of PS which has significantly larger parameter a_{Si} = 0.5431 nm in comparison with Ni.[17]

The initial stages of the electrochemical processing are accompanied by formation of nickel silicide Ni_2Si (111) as its peaks at 2θ 33° are clearly defined on the XRD patterns corresponded to 5 and 15 minutes of Ni deposition (Fig. 4a, 4b). In addition, there is a

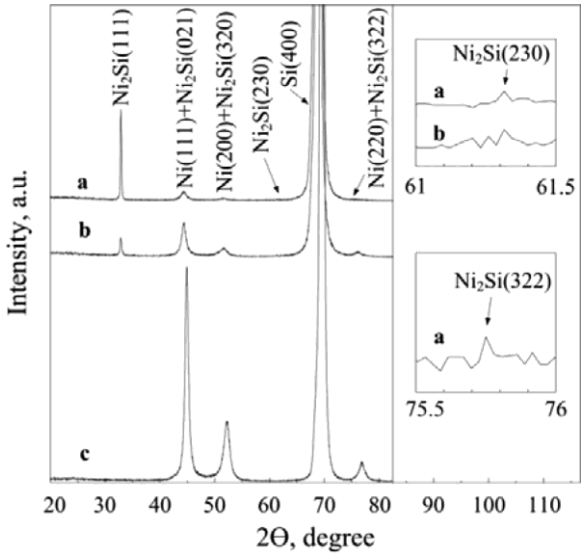

Figure 4. XRD pattern of PS subjected to the Ni electrochemical deposition for 5 (a), 15 (b) and 80(c) minutes.

trace of Ni_2Si (230) reflection at $2\theta \approx 61.3^\circ$ for 5 minutes of the Ni deposition. Moreover, the broadening of the Ni peaks could also be caused by presence of nickel silicide as is mentioned in Figure 4a. The formation of silicide at the metal-silicon interface during high temperature annealing is a well-known fact.[19] For the Ni-Si case nickel diffuse into the Si lattice resulting in a large amount of metallic nonmagnetic phases.[20] Such diffusion process is stimulated by the grain boundaries, surface and bulk defects, temperature.[19]

Generally, the annealing of thin Ni films deposited on Si leads to gradual formation of the three dominant Ni-Si phases. Firstly Ni_2Si is formed at $T \approx 200^\circ C$,[21] which with further increase of temperature up to $400^\circ C$ is converted to the low resistive and less strained monosilicide NiSi. Annealing at higher temperatures leads to the progressive consumption of NiSi by disilicide $NiSi_2$ that fully completes at $T \approx 800^\circ C$.[20] Nevertheless, at the initial stages of Ni deposition on Si substrate, the Ni_2Si disordered islands could be formed even at room temperature.[22] This occurs because the energy released by metal cluster formation can be sufficient to overcome the activation barrier for the diffusion.[23] The room temperature formation of Ni_2Si can be also conditioned by ion beam mixing process.[24,25]

The skeleton of PS used in the present work is known to have a small amount of amorphous silicon (a-Si) with a number of the broken bonds.[26] In our opinion, a-Si represents a favorable material for the Ni diffusion even at room temperature as Ni ions have been found to easily diffuse into Si on its defects.[27]

We suppose that an external electric field provides the concentration of Ni ions near the surface of pore's walls and their further diffusion into the skeleton of PS. However additional energy is required to provide the conversion of the PS surface enriched with Ni ions into nickel silicide. Usually annealing is used for such purposes.[27,28] In our case Ni_2Si most likely is formed due to suitable energetic conditions such as an external electric field and contact potential at the solution/PS interface. On the other hand the energy of the electrochemical system was not enough to provide to the following NiSi and $NiSi_2$ formation as there were no any related peaks on the XRD patterns.

The respective decrease is observed for Ni_2Si (111) peak (Fig. 4b). It is remarkable no peaks of Ni_2Si as well as Ni peaks width decrease were found on the XRD pattern corresponded to 80 minutes of the Ni deposition, i.e. Ni_2Si crystalline phase disappeared (Fig. 4c). Moreover, the increase of the Ni peaks with the increase of the deposition time means the growing amount of Ni was forming simultaneously to the silicide degradation. It indicates the termination of the silicide formation and its progressive conversion to Ni with the prolonged deposition period.

We propose the following mechanism of the complete Ni_2Si decomposition. The silicide growth stops with a lack of the energy of the electrochemical system to overcome the energy barrier needed for the Ni_2Si formation.[29] Ni_2Si is a material of a metallic conductivity and the field of PS/Ni_2Si junction promotes an electron's extraction from the Si skeleton.[30] As Ni_2Si is in the increasing stress on Si while the silicide phase is growing it is favorable to relax and fill with electrons.[29,31] So Ni ions in the silicide layer reduce to the atoms of nickel.

Magnetic properties of Ni deposited in PS.— All the synthesized samples demonstrate ferromagnetic properties. As an example, in Figure 5 we show the measured temperature dependence of the specific magnetization σ of 15 minutes sample. The sample was cooled down to liquid nitrogen temperature and then the constant magnetic field of 8.6 kOe was applied. The magnetization was measured by the static ponderomotive method while heating up to 700 K. The value of the specific magnetization was evaluated by knowing the precise mass of the deposited Ni. The analysis of the results presented in Figure 5 revealed that the absolute value of the low temperature specific magnetization of Ni grown in PS template during 15 minutes ($\sigma \approx 47$ A· m^2· kg^{-1}) is less with respect to low temperature specific magnetization known from the literature for Ni powder (σ 58.9 A· m^2 · kg^{-1}).[32] These measurements allowed obtaining the magnetic moment of Ni atom which equaled to $\mu = 0.49\mu_B$ (where μ_B is the Bohr magneton),

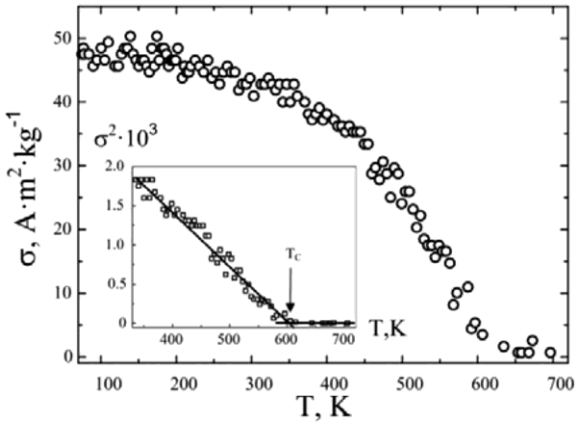

Figure 5. Temperature dependence of the specific magnetization σ for PS template after 15 minutes of Ni deposition. Inset: σ^2 versus temperature dependence. Lines represent linear fits to the experimental data. Arrow indicates the evaluated Curie temperature.

and was also less with respect to the magnetic moment of Ni atom, $\mu = 0.62\mu_B$. In the inset to Figure 5 we plot the σ^2 versus T dependence, which gives the possibility to evaluate the Curie temperature T_C. Indeed, according to the Curie-Weiss theory, the specific magnetization at about T_C depends on temperature as $\sigma \sim (1 - T/T_C)^{1/2}$. From that we obtained $T_C = 597$ K. This value is slightly lower than that known for bulk Ni, $T_C = 627$ K.[33] All these facts confirm the lightly weakened ferromagnetism of Ni at the initial stage of deposition in PS template. The main reason for this is the formation of the nonmagnetic Ni_2Si phase, as follows from the results of XRD analysis (see Fig. 3a, 3b). In this case the loss of electrons of Ni while creating the Ni-Si bonds is especially sensitive to the magnetic properties.

Conclusions

Stationary regime of the nickel electrochemical deposition into the mesoporous silicon template from the Watts bath has been found to obtain continuous Ni NWs. According to the SEM analysis the length and the diameter of NWs have been determined by pore dimensions were equal to 10 μm and 100–120 nm, respectively. The stages of Ni deposition process from nucleation through separated NPs growth to their coalescence in NWs have been carefully studied. The time required for the complete filling of pore channels has been fixed at 60 min of electrochemical deposition. The proposed PS template and regimes of the Ni deposition have allowed achieving the maximum value of the filling factor about 67%. The PS potential during the electrochemical deposition has been found to manifest the filling process of pore volume with Ni. The polycrystalline nature of the Ni NWs has been established by XRD. The lattice parameter of Ni has been determined to be 0.4–0.5% expanded in comparison with the bulk nickel. Such increasing is significant for cubic dense packing of Ni atoms and might be explained by PS matrix influence. Moreover, the formation of nickel silicide Ni_2Si has been observed at the initial stages of Ni deposition. The synthesized PS templates filled with Ni show the magnetic behavior which was proved by measuring the temperature dependence of the specific magnetization. It has been revealed that the specific magnetization and the magnetic moment of Ni atoms, as well as the Curie temperature values are less for sample with the absence of continuous Ni NWs with respect to those known for bulk Ni. We have explained it by formation of nonmagnetic Ni_2Si phase at the initial stages of the deposition.

Further research of the magnetic properties of PS/Ni nanocomposites and their relation to the structure of Ni in PS templates is in progress now.

Acknowledgments

The authors thank V. Tsybulsky for the SEM analysis, V. Petrovich and A. Vecchione for the useful discussions. This research was conducted as a part of the project 2.4.12 of the Belarus Government Research Program "Functional engineering materials, nanomaterials".

References

1. K. Liu, K. Nagodawithana, P. Searson, and C. Chien, *Phys. Rev. B*, **51**, 7381 (1995).
2. M. Tsoi, J. Sun, M. Rooks, R. Koch, and S. Parkin, *Phys. Rev. B*, **69**, 100406(R) (2004).
3. A. Fert and L. Piraux, *J. Magn. Magn. Mater.*, **200**, 338 (1999).
4. R. Ferré, K. Ounadjela, J. M. George, L. Piraux, and S. Dubois, *Phys. Rev. B*, **56**, 14066 (1997).
5. S. Kawai and R. Ueda, *J. Electrochem Soc.*, **122**, 32 (1975).
6. Z. Ye, H. Liu, Z. Luo, H. Lee, W. Wu, D. Naugle, and I. Lyuksyutov, *Nanotechnology*, **20**, 045704 (2009).
7. T. M. Whitney, C. Searson, J. S. Jiang, and C. L. Chien, *Science*, **261**, 1316 (1993).
8. L. Piraux, S. Dubois, E. Ferain, R. Legras, K. Ounadjela, J. M. George, J. L. Maurice, and A. Fert, *J. Magn. Magn. Mater.*, **165**, 352 (1997).
9. R. Herino, P. Jan, and G. Bomchil, *J. Electrochem. Soc.*, **132**, 2514 (1985).
10. R. Herino, in *Properties of Porous Silicon*, L. Canham, Editor, chapter 2.2, INSPEC, London (1997).
11. S. A. Gusev, N. A. Korotkova, D. B. Rozenstein, and A. A. Fraerman, *J. Appl. Phys.*, **76**, 6671 (1994).
12. M. S. Rusetskii, N. M. Kazyuchits, V. G. Baev, A. L. Dolgii, and V. P. Bondarenko, *Pisma Zh. Techn. Fiz.*, **37**, 201 (2011); *Tech. Phys. Letters*, **37**, 391 (2011).
13. S. Aravamudhan, K. Luongo, P. Poddar, H. Srikanth, and S. Bhansali, *Appl. Phys. A*, **87**, 773 (2007).
14. P. Granitzer and K. Rumpf, *Materials*, **3**, 943 (2010); *ibid.*, **4**, 908 (2011).
15. V. I. Chechernikov, *Magnetic measurements*, Moscow, MSU, p. 387 (1969) (in Russian).
16. F. Harraz, T. Sakka, and Y. Ogata, *Phys. Stat. Sol. (a)*, **197**, 51 (2003).
17. International Centre for Diffraction Data, *PCPDFWIN*, *JCPDS*, **2**, 89-838; 85-5648; 81-1936; 01-1242 (1998).
18. H. Pan, H. Sun, C. Poh, Y. Feng, and J. Lin, *Nanotechnology*, **16**, 1559 (2005).
19. V. E. Borisenko, *Semiconducting Silicides*, Springer, 348 p. (2000).
20. K. N. Tu, G. Ottaviani, U. Gösele, and H. Föll, *J. Appl. Phys.*, **54**, 758 (1983).
21. K. N. Tu, *Appl. Phys. Lett.*, **27**, 221 (1975).
22. E. J. van Loeneu, J. W. M. Frenken, and J. F. van der Veen, *Appl. Phys. Lett.*, **45**, 41 (1984).
23. A. Zunger, *Phys. Rev. B*, **24**, 4372 (1981).
24. J. Desimioni and A. Traverse, *Phys. Rev. B*, **48**, 13266 (1993).
25. N. Boussaa, A. Guittoum, and S. Tobbeche, *Vacuum*, **77**, 125 (2005).
26. A. R. Chelyadinsky, A. M. Dorofeev, N. M. Kozuchits, S. L. Monica, S. K. Lazarouk, G. Maiello, G. Masinu, N. M. Penuna, V. F. Stelmakh, V. P. Bondarenko, and A. Ferrari, *J. Electrochem. Soc.*, **144**, 1463 (1997).
27. H. Kim, Y.-J. Yong, J.-L. Lee, and K.-Y. Lee, *J. Mater. Sci. Lett.*, **16**, 560 (1997).
28. K. N. Tu, *Thin Solid Films*, **25**, 403 (1975).
29. K. P. Liew, R. A. Bernstein, and C. V. Thompson, *J. Mater. Res.*, **19**(2), 676 (2004).
30. E. G. Colgan, M. Maenp, M. Finetti, and M-A. Nicolet, *J. El. Mater.*, **12**(2), 413 (1983).
31. D. Mangelinck and K. Hoummada, *Appl. Phys. Lett.*, **92**, 254101 (2008).
32. R. Pauthenet, *High Field Magnetism*, Ed. M. Dafe, Amsterdam, North-Holland Publ. Comp. p. 77 (1983).
33. N. W. Ashcroft and N. D. Mermin, *Solid State Physics*, Saunders College Publishing (1976).